Letters

A Novel Data Generation and Quantitative Characterization Method of Motor Static Eccentricity With Adversarial Network

Wei Sun, *Member, IEEE*, Haowen Wang, and Ronghai Qu, *Fellow, IEEE*

***Abstract*—Eccentricity can cause motor damage. It is necessary to obtain the degree of motor eccentricity for health management or eccentricity suppression. Due to the complex electromagnetic mechanism, it is hard to obtain the degree of motor eccentricity in traditional way. The neural network is suitable for obtaining the degree of eccentricity, but the eccentricity data are too few to train network. In this article, a data generation and quantitative characterization method for motor eccentricity based on improved generative adversarial network is proposed. The mathematical model is improved for pretraining, and the network and objective function are improved for data generation and eccentricity characterization. The results show the validity of the proposed method.**

***Index Terms*—Data generation, eccentricity, generative adversarial network (GAN), physics informed.**

I. Introduction

BECAUSE of the manufacturing errors and unbalance load, rotor eccentricity exits in almost all motors [1]. In industrial application, the acceptable distribution of eccentricity is usually within 10%, and eccentricity is treated as a fault when it is more than 10% [2]. Eccentricity can cause unbalanced magnetic pull, which results in vibration, acoustic noise, and bearing fault, even causes rotor–stator rub [3], [4]. It is important to characterize eccentricity quantitatively for motor health management.

With the development of artificial intelligence, neural network (NN) is widely used in eccentricity characterization. In [5], to characterize the eccentricity of line start permanent magnet synchronous motors, the principal component analysis (PCA) is used to extract the features from stator current, then the features are as input to NN for eccentricity quantitative characterization. In [6], the sideband frequency components of current are as input to network, and the output is the eccentricity degree of permanent magnet synchronous motors. As a data driven model, large number of data are needed for network training. Considering almost all motors are normal (within 10% eccentricity), it is hard to obtain data under different eccentricity degrees in actual. In addition, the eccentricity degree is difficult to be measured, so the data are unlabeled and cannot be used for network training.

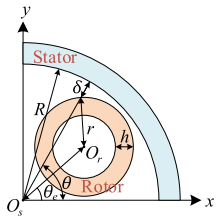

Fig. 1. Diagram of PMSM with eccentricity.

There are few methods to deal with the data lacking problem in eccentricity characterization. In this article, a data generation and quantitative characterization method for motor eccentricity based on improved generative adversarial network (GAN) is proposed. The data from actual motor are combined with model data to train the GAN, then the generated data can be used for eccentricity characterization. The innovations are as follows.

1) The mathematical model of permanent magnet synchronous motor (PMSM) is analyzed for constructing the eccentricity features and static eccentricity (SE) quantitative characterization.
2) An adversarial network is proposed to adapt to data generation of different eccentricity degrees, with only unlabeled normal data (within 10% eccentricity) training. It can solve the data lacking problem in motor eccentricity characterization.
3) To better measure the differences between the generated and actual electromotive force (EMF), GAN is improved to be dual channel. In addition, the penalty term is added to the objective function in adversarial training to avoid overtuning.

II. Mathematical Model

A. Analysis of Air-Gap

For SE, the air-gap length is uneven around the rotor. According to the geometric relationship shown in Fig. 1, the air-gap

Manuscript received 15 February 2023; revised 20 March 2023; accepted 9 April 2023. Date of publication 17 April 2023; date of current version 19 May 2023. This work was supported by the Delta Power Electronics Science and Education Development Program of Delta Group under Grant DREK2021003. *(Corresponding author: Wei Sun.)*

The authors are with the School of Electrical and Electronic Engineering, Huazhong University of Science and Technology, Wuhan 430074, China (e-mail: sunwei77@hust.edu.cn; m202171935@hust.edu.cn; ronghaiqu@hust.edu.cn).

Data is available on-line at https://github.com/HaowenWang98/StaticEccentricity.

Color versions of one or more figures in this article are available at https://doi.org/10.1109/TPEL.2023.3267883.

Digital Object Identifier 10.1109/TPEL.2023.3267883

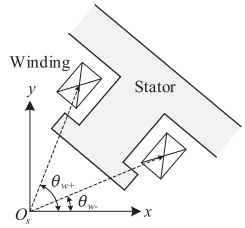

Fig. 2. Diagram of one stator winding.

length at θ is expressed as follows:

$$\delta(\theta) = R - |O_s O_r| \cos(\theta - \theta_e) - \sqrt{r^2 - |O_s O_r|^2 \sin(\theta - \theta_e)} \tag{1}$$

where R is the inner radius of stator, r is the outer radius of rotor, and θ_e is the eccentricity angle. O_s and O_r are the center of stator and rotor, respectively. Considering the eccentric distance $|O_s O_r|$ is greatly shorter than the outer radius of rotor r, and the absolute value of sine function is limited to 0 to 1, (1) can be approximated as follows:

$$\delta(\theta) \approx \delta_0 [1 - \varepsilon \cos(\theta - \theta_e)] \tag{2}$$

where δ_0 is the air-gap length without eccentricity. $\varepsilon = |O_s O_r|/\delta_0$ is the eccentricity degree, which reflects the degree of eccentricity [7].

Assuming the air-gap flux density distributes sinusoidally, it can be expressed as follows:

$$B_h(\theta) = B \cos[p(\phi - \theta)] \tag{3}$$

where p is the number of pole pairs, B is the amplitude of the air-gap flux density, and ϕ is the position of rotor pole. According to the inversely proportional relationship between air-gap length and flux density, the air-gap flux density with eccentricity can be expressed as follows:

$$B_e(\theta) = \frac{\delta_0 + h}{\delta(\theta) + h} B_h(\theta) \tag{4}$$

where h is the height of permanent magnet.

B. Eccentric EMF Model

Some researchers have analyzed the flux density of eccentric motor [8]. However, it is difficult to measure it directly in practical and construct features. In this section, the EMF model is analyzed based on the flux density and the amplitudes of EMF on each winding are used to construct feature vector.

Considering the winding shown in Fig. 2, according to electromagnetic induction law, the EMF of this winding can be expressed as follows:

$$E_w = N l w_r R B_e(\theta_{w+}) - N l w_r R B_e(\theta_{w-}) \tag{5}$$

where N is the number of turns per winding and l is the axial length. Taking (2)–(4) into (5), replacing ϕ with $\omega_r t + \phi_0$, the back EMF at time t can be expressed as follows:

$$E = N l B w_r R (h + \delta_0) \left\{ \frac{\cos[p(w_r t + \phi_0 - \theta_{w+})]}{h + \delta_0 [1 - \varepsilon \cos(\theta_{w+} - \theta_e)]} - \frac{\cos[p(w_r t + \phi_0 - \theta_{w-})]}{h + \delta_0 [1 - \varepsilon \cos(\theta_{w-} - \theta_e)]} \right\} \tag{6}$$

where ϕ_0 is the initial value of ϕ. According to (6), the EMF under different SE degrees can be obtained. In addition, the amplitude of back EMF can be expressed as follows:

$$|E| = (h + \delta_0) N B l \omega_r R \left[\left(\frac{1}{h + \delta_0 [1 - \varepsilon \cos(\theta_{w+} - \theta_e)]} \right)^2 + \left(\frac{1}{h + \delta_0 [1 - \varepsilon \cos(\theta_{w-} - \theta_e)]} \right)^2 - \frac{2 \cos[p(\theta_{w+} - \theta_{w-})]}{(h + \delta_0 [1 - \varepsilon \cos(\theta_{w+} - \theta_e)])(h + \delta_0 [1 - \varepsilon \cos(\theta_{w-} - \theta_e)])} \right]^{\frac{1}{2}}. \tag{7}$$

It can be seen that, the eccentricity degree ε is contained in the amplitude, which can be used for eccentricity quantitative characterization.

III. Data Generation Method

A. Brief of GAN

GAN was originally proposed in 2014, which is inspired by zero-sum game [9]. GAN aims to create real image data from noise data, and the generator G is applied to map the random noise z to image data x. The goal of discriminator D is to identify whether the data are generated. The objective function of GAN can be expressed as follows:

$$\min_G \max_D V = -E_{x \sim X}[\log D(x)] - E_{x \sim z}[\log(1 - D(G(z)))] \tag{8}$$

B. Proposed Data Generation Method

There is a dilemma. The model data are many but inaccurate, and the actual data are accurate but few. To obtain large number of accurate data, the model data and actual data are combined to train the network.

Traditional GAN needs large amount of data for training. However, the actual eccentricity data are few, and only distribute within 10% eccentricity. Therefore, the GAN needs to be improved. In this article, a pretraining method for the generator is proposed, and the penalty term is added to the objective function in adversarial training to avoid overtuning. In addition, the discriminator is improved to be dual channel to measure the differences better. The details of improvements are as follows.

1) Due to lacking of data, the generator needs to be pretrained by model data to be initialized approximately, then it is fine-tuned by adversarial training to generate accurate data. Within pretraining, the generator is trained by different eccentricity model data, which can reflect the different eccentricity electromagnetic law [10], [11], so the generator can learn similar features from model data, and these features are helpful to improve the performance of network on actual data. Therefore, with the pretraining, the fine-tuned network still can perform well because it

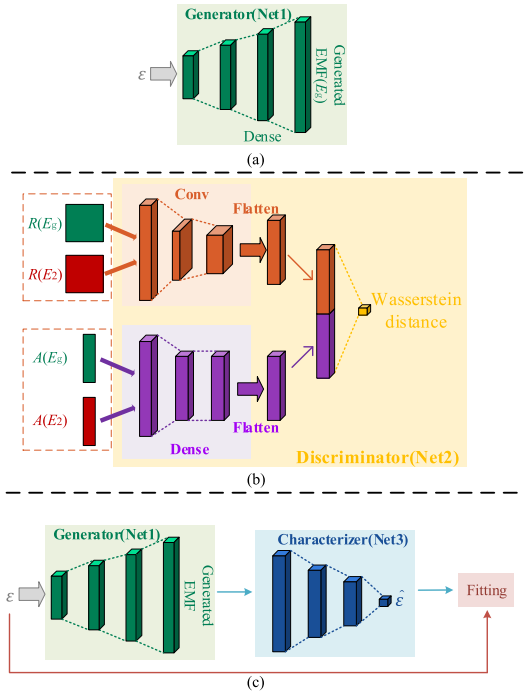

Fig. 3. Structure of dual channel Wasserstein GAN. (a) Pretraining. (b) Adversarial training. (c) Fitting.

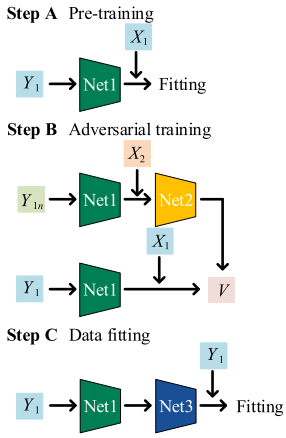

Fig. 4. Diagram of network training.

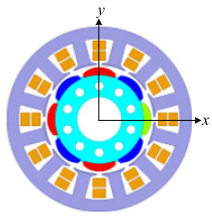

Fig. 5. Structure of 12s8p PMSM.

has obtained much prior knowledge from the model data, although the actual data are restricted.

2) To better measure the differences between the generated and actual EMF, the discriminator is improved to be dual channel to extract relative and absolute features.
3) To stabilize the training process, avoid model collapse and gradient disappearance. Wasserstein distance [12] is used to measure the differences between generated data and actual data. Wasserstein distance can describe the distance of the two distributions, no matter how the two distributions are overlapped or not, but conventional GANs cannot describe the distance when there is no overlap in the two distributions [13]. In addition, to avoid overtuning, the penalty term is added to the objective function, which can be expressed as follows:

$$\min_G \max_D V = E\left\{D_w\left[G\left(\varepsilon_{1n}^i\right)\right]\right\} - E\left[D_w\left(E_2^i\right)\right] + \lambda \cdot E\left\{S\left[G\left(\varepsilon_1^i\right) - E_1^i\right]\right\} \tag{9}$$

where $D_w(\cdot)$ is the Wasserstein discriminator, $E(\cdot)$ is the sample expectation, and $S(\cdot)$ is the variance. λ is the penalty weight.

The structure of dual channel Wasserstein GAN is shown in Fig. 3, and the diagram of network training is shown in Fig. 4. $X_1 = \{E_1^i\}_{i=1}^{m_1}$ and $Y_1 = \{\varepsilon_1^i\}_{i=1}^{m_1}$ represent model data and corresponding eccentric information, respectively. Y_{1n} represent the normal part (within 10% eccentricity) of Y_1.$X_2 = \{E_2^i\}_{i=1}^{m_2}$ represents the actual data (collected from actual motor, within 10% eccentricity).

In step A, the generator is pretrained by the model data. The eccentricity degree is as input to generator, and the outputs of the generator are the back EMF amplitudes on each winding. Then, implementing step B to realize adversarial training. Finally, the characterizer is used to fit generated data in step C.

In addition, for one sample $E^i = [e^1, e^2, \ldots, e^n]$, the variance can be calculated as follows:

$$S\left(E^i\right) = \frac{1}{n}\sum_{j=1}^{n}\left(e^j - \frac{1}{n}\sum_{k=1}^{n}e^k\right)^2. \tag{10}$$

The absolute feature $A(E^i)$ is the absolute value of E^i, and the relative feature $R(E^i)$ can be calculated as follows:

$$R\left(E^i\right) = \begin{bmatrix} e^1 - e^1 & e^1 - e^2 & \cdots & e^1 - e^n \\ e^2 - e^1 & e^2 - e^2 & \cdots & e^2 - e^n \\ \vdots & \vdots & \ddots & \vdots \\ e^n - e^1 & e^n - e^2 & \cdots & e^n - e^n \end{bmatrix}. \tag{11}$$

IV. Experiment

A. Data Description and Network Configuration

To verify the validity of the proposed method, a 12/8-pole PMSM is used for research. The structure of the PMSM is shown in Fig. 5, and the parameters are shown in Table I. To ease expression, the stator center is selected as origin, and the winding at direction of x-axis is named winding 1, and winding 2∼12 is arrayed anticlockwise.

The structure of SE motor platform is designed, as shown in Fig. 6(a). The rotor is fixed, and the stator is installed to the step motor. Lifting the stator to change the relative position of stator and rotor and SE is set.

TABLE I
SPECIFICATION OF THE PMSM

Parameter	Value	Parameter	Value
Rated speed	3000 rpm	p	4
Rated current	5.7 A	R	49 mm
N	43	r	47 mm
l	75 mm	B	0.83 T
δ_0	2 mm	h	5.5 mm

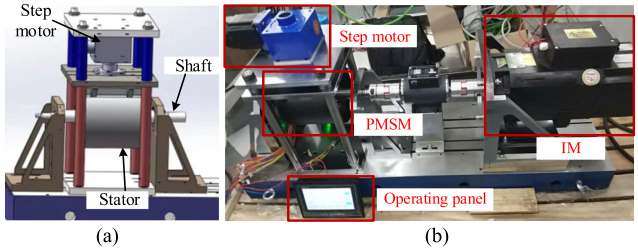

Fig. 6. Design of SE motor platform.

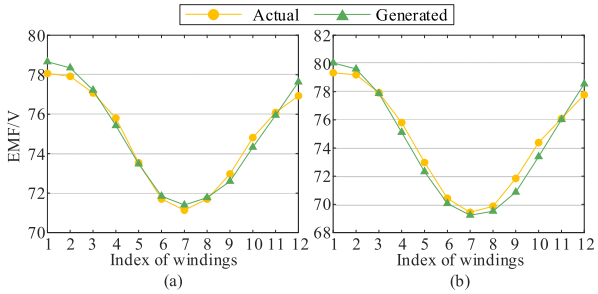

Fig. 7. Generated EMF amplitudes on each winding. (a) Under 20% SE. (b) Under 30% SE.

The platform of PMSM with adjustable eccentricity is shown in Fig. 6(b). Step motor is controlled by operating panel, and the shortest moving distance is 0.25 mm, so the accuracy of SE can reach to 1.25%. The PMSM is dragged by induction motor (IM) to rotate, and the EMF is obtained. In the experiments, the data are collected under rated speed.

For the network, there are two hidden layers in Net1. For Net2, the dense part contains two hidden layers, and the convolutional part contains two convolutional layers and two pool layers.

B. Data Generation and SE Quantitative Characterization

To verify that the proposed method is valid, the generated EMF amplitudes on each winding are shown in Fig. 7. It can be seen that the generated data are accurate under different SE degrees. It indicates that the proposed method can generate data under different SE degrees based on only normal data, which solves the data lacking problem.

Then, the generated data are used to train the characterizer for SE characterization. The data collected from SE motor platform are as input to characterizer, and the results of SE characterization are shown in Fig. 8. To quantify the performance of the proposed method, the absolute errors of each sample are shown in the bottom of the figure. It can be seen

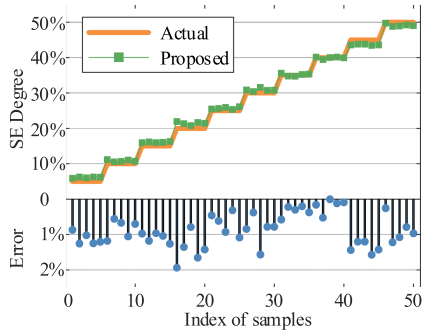

Fig. 8. Results of SE characterization by proposed data generation method.

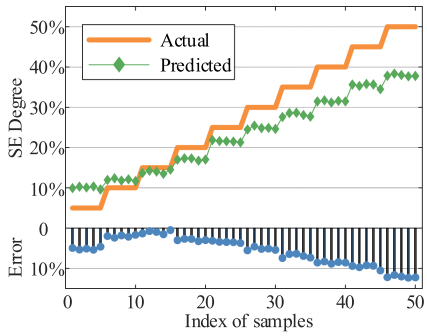

Fig. 9. Results of characterizer trained by only model data.

that the errors of the characterization results are almost within 2%, and the characterized results are close to the actual values. The results mean the generated EMFs are useful for eccentricity characterization.

The characterizer trained by only model data (X_1 and Y_1) is used for comparison, and the results are shown in Fig. 9. It is obvious that the errors are larger than the proposed method, which means the eccentricity characterization based on only model data is inaccurate. In addition, due to lacking of label, it is impractical to characterize eccentricity using actual data directly. The results reflect the validity and necessity of the proposed method.

C. Selection of Parameter

Considering that the generated data are approximately close to the actual after pretraining, the penalty term is used to constrain the tuning of generator in adversarial training. To measure the influence of penalty term, the mean absolute percentage errors (MAPEs) of generated EMFs are selected to quantify the performance, which can be calculated as

$$\text{MAPE} = \frac{1}{m}\sum_{i=1}^{m}\frac{\left|\hat{y}^i - y^i\right|}{y^i} \tag{12}$$

where y^i and $\hat{y}^i$ are the actual value and output of generator, respectively. The MAPEs of generated EMFs under different penalty weights are shown in Fig. 10. According to (9), the larger the penalty term is, the generated data are similar to the model data, the more the generator constrained. But it is overtuning

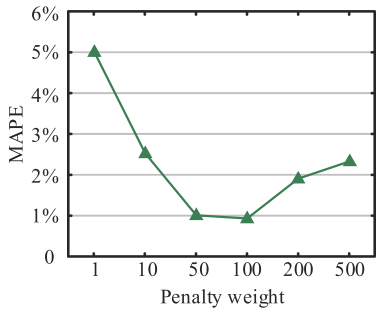

Fig. 10. MAPEs of generated EMFs under different penalty weights.

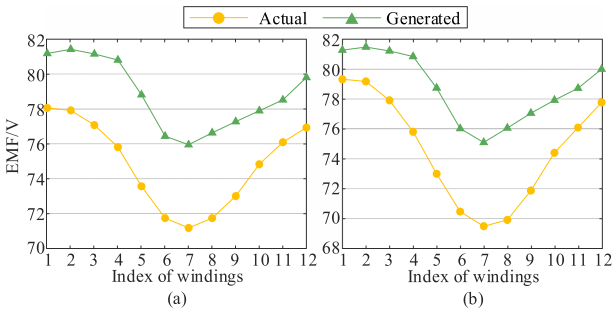

Fig. 11. Generated EMF amplitudes on each winding without penalty term ($\lambda = 0$). (a) Under 20% SE. (b) Under 30% SE.

TABLE II
COMPARISON WITH RELATED METHODS

Method	Accuracy	Eccentricity step
PCA+NN[5]	95.6%	10%
KNN+NN[6]	99.31%	10%
TFR+NN-HMM[14]	100%	20%
Proposed	100%	5%

when the weight is small. Both of them cause the high error. According to the results, 100 is selected as the weight.

To further discuss the importance of the penalty term, the results of data generation without penalty term ($\lambda = 0$) are shown in Fig. 11. It can be seen that the generated EMF amplitudes are far from the actual data when the penalty weight is too small. On the contrary, due to the restriction of the penalty term, the generated data can only be changed slightly to keep the loss low, and the results in Fig. 7 are close to the actual data. It also proves that the proposed method can avoid overtuning.

D. Comparison With Related Methods

To further evaluate the performance, the proposed method is compared with related methods of eccentricity characterization. In the related work [5], [6], [14], the accuracy (percentage of the correctly classified samples) and eccentricity step (the minimum interval of eccentricity degree classification) are employed as the criteria, and the criteria in this article are same as the related work. The results are given in Table II.

In [5], PCA is employed to extract fault features from the line current, and the selected components are input to NN to recognize the SE severity, finally, 95.6% accuracy was achieved as 10% step. In [6], the eccentricity type of the PMSM is first classified by k-nearest neighbor (KNN) classifier, and then, the sideband frequency components of current are as input to network for eccentricity severity prediction. The average accuracy of the method reached to 99.31%. In [14], the current measurements based on nonparametrical time–frequency representation (TFR) are used for features extraction, and the features are input to neural network and hidden Markov model together (NN-HMM) to recognize eccentricity degree. This method achieved to 100% accuracy on the IM as 20% step.

To compared with the abovementioned methods, the characterization results of proposed method are classified to different degrees as 5% eccentricity step (for example, the characterization result that between 7.5% and 12.5% is classified to 10% eccentricity degree). According to the results shown in Fig. 8, the maximum error is below 2%, so the proposed method can achieve 100% accuracy under 5% step. Comparing with the abovementioned methods, it can be concluded that: 1) the proposed method can achieve better accuracy under smaller eccentricity step, and 2) the proposed method is only trained by normal data, it is more practical.

V. CONCLUSION

To solve the data lacking problem for eccentricity characterization, a data generation method is proposed. First, the model of eccentric PMSM is obtained, which indicates that the EMF amplitude can be used for SE characterization. Then, the model data are combined with actual data to train the generator. Finally, the generated data are used for characterizer training. The experimental results show that the method can generate accurate data, and these data can be used for eccentricity characterization.

REFERENCES

[1] Y.-L. He et al., "A new external search coil based method to detect detailed static air-gap eccentricity position in nonsalient pole synchronous generators," *IEEE Trans. Ind. Electron.*, vol. 68, no. 8, pp. 7535–7544, Aug. 2021, doi: 10.1109/TIE.2020.3003635.

[2] S. Nandi, T. C. Ilamparithi, S. B. Lee, and D. Hyun, "Detection of eccentricity faults in induction machines based on nameplate parameters," *IEEE Trans. Ind. Electron.*, vol. 58, no. 5, pp. 1673–1683, May 2011.

[3] J. Ren, X. Wang, and W. Zhao, "Magnetic field prediction of the saturated surface-mounted permanent magnet synchronous machine with rotor eccentricity," *IEEE Trans. Ind. Electron.*, vol. 69, no. 8, pp. 7756–7766, Aug. 2022.

[4] U. Galfarsoro, A. Mccloskey, S. Zarate, X. Hernandez, and G. Almandoz, "Influence of manufacturing tolerances and eccentricities on the unbalanced magnetic pull in permanent magnet synchronous motors," *IEEE Trans. Ind. Appl.*, vol. 58, no. 3, pp. 3497–3510, May/Jun. 2022.

[5] I. M. Hussein and Z. Al-Hamouz, "Neural network based detection technique for eccentricity fault in LSPMS motors," in *Proc. Innovations Intell. Syst. Appl. Conf. (ASYU)*, 2018, pp. 1–5.

[6] B. M. Ebrahimi, J. Faiz, and M. J. Roshtkhari, "Static-, dynamic-, and mixed-eccentricity fault diagnoses in permanent-magnet synchronous motors," *IEEE Trans. Ind. Electron.*, vol. 56, no. 11, pp. 4727–4739, Nov. 2009, doi: 10.1109/TIE.2009.2029577.

[7] Q. Xu, S. Yuan, X. Liu, P. W. T. Pong, and C. Liu, "Online detection and location of eccentricity fault in PMSG with external magnetic sensing," *IEEE Trans. Ind. Electron.*, vol. 69, no. 10, pp. 9749–9760, Oct. 2022.

[8] J. J. Pérez-Loya, C. J. D. Abrahamsson, and U. Lundin, "Electromagnetic losses in synchronous machines during active compensation of unbalanced magnetic pull," *IEEE Trans. Ind. Electron.*, vol. 66, no. 1, pp. 124–131, Jan. 2019.

[9] I. Goodfellow et al., "Generative adversarial nets," in *Proc. Adv. Neural Inf. Process. Syst.*, 2014, pp. 2672–2680. [Online]. Available: http://papers.nips.cc/paper/5423-generative-adversarial-nets.pdf

[10] A. J. Piña Ortega and L. Xu, "Investigation of effects of asymmetries on the performance of permanent magnet synchronous machines," *IEEE Trans. Energy Convers.*, vol. 32, no. 3, pp. 1002–1011, Sep. 2017, doi: 10.1109/TEC.2017.2684165.

[11] Z. J. Liu and J. T. Li, "Accurate prediction of magnetic field and magnetic forces in permanent magnet motors using an analytical solution," *IEEE Trans. Energy Convers.*, vol. 23, no. 3, pp. 717–726, Sep. 2008, doi: 10.1109/TEC.2008.926034.

[12] J. Li, Y. Zi, Y. Wang, and Y. Yang, "Health indicator construction method of bearings based on Wasserstein dual-domain adversarial networks under normal data only," *IEEE Trans. Ind. Electron.*, vol. 69, no. 10, pp. 10615–10624, Oct. 2022.

[13] W. Hu, T. Wang, and F. Chu, "Fault feature recovery with wasserstein generative adversarial imputation network with gradient penalty for rotating machine health monitoring under signal loss condition," *IEEE Trans. Instrum. Meas.*, vol. 71, 2022, Art. no. 3511812, doi: 10.1109/TIM.2022.3168898.

[14] I. Bouchareb, A. Lebaroud, A. J. M. Cardoso, and S. B. Lee, "Towards advanced diagnosis recognition for eccentricities faults: Application on induction motor," *IEEE 12th Int. Symp. Diagnostics Elect. Mach., Power Electron. Drives*, pp. 271–282, 2019, doi: 10.1109/DEMPED.2019.8864920.